

Third-Order Elastic Constants of NaCl and KCl Single Crystals*†

ZUNG-PING CHANG‡

Department of Physics, Rensselaer Polytechnic Institute, Troy, New York

(Received 14 June 1965)

Measurements have been made to determine the third-order elastic constants of NaCl and KCl single crystals. The relations between the velocities of ultrasonic waves propagating along the $[1\bar{1}0]$ and $[\bar{1}\bar{1}2]$ directions under a uniaxial compression applied in the $[111]$ direction and the elastic constants were derived. Six velocities of these ultrasonic waves were then measured at room temperature as functions of the strain using the pulsed-ultrasonic-interference technique. From the present measurements under the (111) compression and those under the hydrostatic pressure by Lazarus, eleven equations were obtained for both NaCl and KCl crystals. From these equations, the following five constants (Brugger's definition for the third-order elastic constants) in units of 10^{12} dyn/cm² were solved by the method of least squares:

	$C_{111}+2C_{112}$	$C_{111}-C_{123}$	C_{456}	C_{144}	C_{166}
NaCl	-9.91 ± 0.04	-9.10 ± 0.08	0.271 ± 0.014	0.257 ± 0.016	-0.611 ± 0.007
KCl	-7.44 ± 0.01	-7.15 ± 0.02	0.118 ± 0.004	0.127 ± 0.005	-0.245 ± 0.002

The Cauchy relation $C_{456} = C_{144}$ is seen to be satisfied to within the probable error in both NaCl and KCl crystals at room temperature. By assuming the validity of the other two Cauchy relations, one can estimate the constants C_{111} , C_{112} , and C_{123} as follows:

	C_{111}	C_{112}	C_{123}
NaCl	-8.80	-0.571	0.284
KCl	-7.01	-0.224	0.133.

I. INTRODUCTION

THE third-order elastic constants are quantities of interest because they relate to the anharmonic properties of the crystal lattices. Their values determine in the long-wavelength limit the phonon-phonon coupling which limits the thermal relaxation time. They also contribute to the thermal expansion and to the lattice specific heat at temperatures higher than the Debye characteristic temperature. They are manifest in the nonlinear properties of sound waves in a solid, e.g., the second harmonic generation,¹ the intersection of two sound beams to generate a third beam,² and the asymmetry in the diffraction pattern formed by passing monochromatic light through a cubic crystal perpendicular to the direction of a sound wave.³

In determining the third-order elastic constants, we have chosen the direct method of observing the change of sound velocity in a solid under compression. Accurate velocity measurement is necessary since the velocity change is usually small in the available stress range. The use of an interference method enables the detection of quite small changes in the velocity and opens the way for the measurement of the third-order elastic constants.

* This work is based on a portion of a thesis submitted in partial fulfillment of the requirements for the Ph.D. degree at Rensselaer Polytechnic Institute, 1964.

† Supported by the National Aeronautics and Space Administration, and by the National Science Foundation.

‡ Present address: Materials Research Laboratory, The Pennsylvania State University, University Park, Pennsylvania.

¹ M. A. Breazeale and D. O. Thompson, *Appl. Phys. Letters* **3**, 77 (1963).

² F. R. Rollins, *Appl. Phys. Letters* **2**, 147 (1963).

³ J. Melngailis, A. A. Maradudin, and A. Seeger, *Phys. Rev.* **131**, 1972 (1963).

So far the variation of sound velocity with stress has mostly been measured under hydrostatic pressure. In order to obtain the complete set of the third-order elastic constants of a material, other conditions of stress, such as uniaxial compression, have to be applied. The difficulty lies in that even a low uniaxial stress can initiate slip and plastic deformation, and the dislocations generated by such flow will cause large effects that mask the true third-order constants of the bulk material. Up to the present, very few measurements have been made to determine the whole set of the third-order elastic constants. The first measurement was made by Hughes and Kelly⁴ (1953) who determined the three independent third-order elastic constants of the isotropic materials polystyrene, Pyrex, and Armco iron. In 1961, Bateman, Mason, and McSkimin⁵ determined the six independent third-order elastic constants of germanium, a first experiment of this kind on a cubic material.

Alkali halides are substances of interest from the theoretical point of view because a simple model of their structure has been quite successful. No complete determination of their six independent third-order elastic constants has yet been made. The variation of elastic constants with pressure has, however, been measured by Lazarus⁶ (1949) and Bartels⁷ (1964).

Although there are many easy-slip systems in NaCl-type alkali halides, the resolved shear stresses in the primary easy-slip directions, $\langle 110 \rangle$ in the slip planes

⁴ D. S. Hughes and J. L. Kelly, *Phys. Rev.* **92**, 1145 (1953).

⁵ T. Bateman, W. P. Mason, and H. J. McSkimin, *J. Appl. Phys.* **32**, 928 (1961).

⁶ D. Lazarus, *Phys. Rev.* **76**, 545 (1949).

⁷ R. A. Bartels, U. S. Office of Naval Research Technical Report No. 8, 1964 (unpublished).

{110} are zero for uniaxial stress applied in a [111] direction. For this orientation of stress, the elastic range in which one can make measurements without yielding is considerably extended.

II. THEORY

In the present paper, Brugger's definition of the third-order elastic constants⁸ is used. With his definition, the strain energy ϕ in a cubic lattice can be expressed in terms of the strain components as

$$\begin{aligned} \phi = & \frac{1}{2}C_{11}(\eta_{11}^2 + \eta_{22}^2 + \eta_{33}^2) + C_{12}(\eta_{11}\eta_{22} + \eta_{22}\eta_{33} + \eta_{33}\eta_{11}) \\ & + C_{44}(\eta_{12}^2 + \eta_{21}^2 + \eta_{23}^2 + \eta_{32}^2 + \eta_{31}^2 + \eta_{13}^2) \\ & + \frac{1}{6}C_{111}(\eta_{11}^3 + \eta_{22}^3 + \eta_{33}^3) \\ & + \frac{1}{2}C_{112}\{\eta_{11}^2(\eta_{22} + \eta_{33}) + \eta_{22}^2(\eta_{33} + \eta_{11}) + \eta_{33}^2(\eta_{11} + \eta_{22})\} \\ & + C_{123}\eta_{11}\eta_{22}\eta_{33} + C_{456}(\eta_{12} + \eta_{21})(\eta_{23} + \eta_{32})(\eta_{31} + \eta_{13}) \\ & + C_{144}\{\eta_{11}(\eta_{23}^2 + \eta_{32}^2) + \eta_{22}(\eta_{13}^2 + \eta_{31}^2) + \eta_{33}(\eta_{12}^2 + \eta_{21}^2)\} \\ & + C_{166}\{(\eta_{11} + \eta_{22})(\eta_{12}^2 + \eta_{21}^2) + (\eta_{22} + \eta_{33})(\eta_{23}^2 + \eta_{32}^2) \\ & \quad + (\eta_{33} + \eta_{11})(\eta_{31}^2 + \eta_{13}^2)\}, \quad (1) \end{aligned}$$

where η_{ij} are the components of the Lagrangian strain which are defined in the following matrix equation⁹:

$$[\eta] = \frac{1}{2}[\tilde{J}J - E]. \quad (2)$$

Here, J is the Jacobian relating the final position of a particle in the lattice after deformation and its initial position, and E is a unit matrix of rank 3.

For the convenience of comparison with the expressions in other literatures, the relations between the C_{ijk} defined by Brugger (C_{ijk}^{Br}) and by Birch¹⁰ (C_{ijk}^{Bi}) are listed below¹¹:

$$\begin{aligned} C_{111}^{Br} &= 6C_{111}^{Bi}, & C_{112}^{Br} &= 2C_{112}^{Bi}, & C_{123}^{Br} &= C_{123}^{Bi} \\ C_{456}^{Br} &= \frac{1}{4}C_{456}^{Bi}, & C_{144}^{Br} &= \frac{1}{2}C_{144}^{Bi}, & C_{166}^{Br} &= \frac{1}{2}C_{166}^{Bi}. \end{aligned}$$

For the stress applied in the [111] crystallographic direction, it is easier to transform the calculation in a new coordinate system with the 1', 2', and 3' axes in the [111], [110], and [112] directions, respectively. Hereafter, a single prime will be used to denote the quantities referred to the new coordinate system. The transform matrix $[R]$ relating these two coordinate systems by the matrix equation

$$\begin{bmatrix} x' \\ y' \\ z' \end{bmatrix} = [R] \begin{bmatrix} x \\ y \\ z \end{bmatrix}$$

is found to be

$$[R] = \begin{bmatrix} 1/\sqrt{3} & 1/\sqrt{3} & 1/\sqrt{3} \\ -1/\sqrt{2} & 1/\sqrt{2} & 0 \\ -1/\sqrt{6} & -1/\sqrt{6} & 2/\sqrt{6} \end{bmatrix}. \quad (3)$$

⁸ K. Brugger, Phys. Rev. **133**, A1611 (1964).
⁹ T. D. Murnaghan, *Finite Deformation of an Elastic Solid* (John Wiley & Sons, Inc., New York, 1951).
¹⁰ F. Birch, Phys. Rev. **71**, 809 (1947).
¹¹ The relation between Birch's C_{456} and Brugger's C_{456} should be $C_{456}^{Br} = \frac{1}{4}C_{456}^{Bi}$, not $\frac{1}{8}$ as obtained from Eq. (13) in Brugger's paper (Ref. 8); if the C_{456} term in the expression of the strain energy is $C_{456}(\eta_{12}\eta_{23}\eta_{31} + \eta_{21}\eta_{32}\eta_{13})$ as it is in Birch's paper (Ref. 10).

The relation between the strains in the two coordinate system is

$$[\eta] = [\tilde{R}][\eta'] [R] \quad \text{or} \quad [\eta'] = [R][\eta][\tilde{R}]. \quad (4)$$

As in Birch's analysis,¹⁰ let us consider a deformation in which the final position (x'_1, x'_2, x'_3) of a particle initially at (a'_1, a'_2, a'_3) is given by

$$[x'] = [A'][a'] + [U'(a', t)] \quad (5)$$

where $[x']$, $[a']$, and $[U'(a', t)]$ are column vectors standing, respectively for the final, the initial position, and an infinitesimal displacement which is a general function of the initial position a' and the time t , and $[A']$ is a 3x3 matrix describing a finite-homogeneous deformation due to an initial stress. From (5), the Jacobian

$$\partial(x'_1, x'_2, x'_3) / \partial(a'_1, a'_2, a'_3)$$

and hence the Lagrangian strain η can be calculated.

If one takes into account the fact that the three cubic axes are equivalent with respect to the [111] direction, then for a uniaxial stress in the [111] direction, the suffixes 1, 2, and 3 in η_{ij} are interchangeable, i.e., $\eta_{11} = \eta_{22} = \eta_{33}$ and $\eta_{12} = \eta_{23} = \eta_{31}$, and from (4) one can show $\eta_{11}' = \eta_{11} + 2\eta_{12}$, $\eta_{22}' = \eta_{33}' = \eta_{11} - \eta_{12}$ and $\eta_{12}' = \eta_{23}' = \eta_{31}' = 0$. Hence, the 1', 2', and 3' axes form a set of principal axes with the strain being isotropic in the plane normal to 1' axis, and thus the matrix A' is diagonal with $A_{22}' = A_{33}'$. The Lagrangian strain $\eta_{ij}'^{(0)}$ resulting from this initial uniaxial stress are

$$\begin{aligned} \eta_{11}'^{(0)} &= \frac{1}{2}(A_{11}'^2 - 1) \equiv \alpha_1, \\ \eta_{22}'^{(0)} &= \eta_{33}'^{(0)} = \frac{1}{2}(A_{22}'^2 - 1) \equiv \alpha_2, \\ \eta_{ij}'^{(0)} &= 0 \quad \text{for } i \neq j. \end{aligned} \quad (6)$$

In the finite-deformation theory, the stress and the strain are related by⁹

$$[T'] = (\rho_x / \rho_0) [J'] [\partial \phi(\eta') / \partial \eta'] [\tilde{J}'], \quad (7)$$

where $[T']$ is the stress tensor, ρ_0 and ρ_x are the initial and the final density, respectively.

For an initial stress $-t$ (t positive for compression) in the [111] direction, the stress tensor $[T']$ is

$$\begin{bmatrix} -t & 0 & 0 \\ 0 & 0 & 0 \\ 0 & 0 & 0 \end{bmatrix}.$$

The values α_1 and α_2 of the Lagrangian strain $\eta_{11}'^{(0)}$ and $\eta_{22}'^{(0)}$ can be found from the two linearly independent equations in (7):

$$\begin{aligned} \frac{1 + 2\alpha_2}{(1 + 2\alpha_1)^{1/2}} t &= \frac{1}{3}(C_{11} + 2C_{12})\theta + \frac{1}{3}C_{44}\delta \\ &+ [(1/18)C_{111} + \frac{1}{3}C_{112} + \frac{1}{3}C_{123}]\theta^2 \\ &+ (8/9)C_{456}\delta^2 + \frac{2}{3}C_{144}\delta(\alpha_1 + \alpha_2) \\ &\quad + \frac{1}{3}C_{166}\delta(\alpha_1 + \alpha_2), \\ 0 &= \frac{1}{3}(C_{11} + 2C_{12})\theta - \frac{2}{3}C_{44}\delta \\ &+ [(1/18)C_{111} + \frac{1}{3}C_{112} + \frac{1}{3}C_{123}]\theta^2 \\ &\quad - (4/9)C_{456}\delta^2 - \frac{2}{3}C_{144}\delta\alpha_2 - \frac{1}{3}C_{166}\delta\alpha_2, \end{aligned}$$

where

$$\theta \equiv \alpha_1 + 2\alpha_2, \quad \delta \equiv \alpha_1 - \alpha_2. \quad (8)$$

The Poisson ratio σ for the strain perpendicular to $[111]$ direction with the stress in $[111]$ direction is $-(\alpha_2/\alpha_1)$ which for the present approximation can be obtained from (8) by neglecting the second- and higher-order terms of α_i , since σ will appear in the first-order terms of α_i in the expressions of $\rho_0 V^2$ to be shown later. The result is then

$$\sigma = (C_{11}^\theta + 2C_{12}^\theta - 2C_{44}^\theta) / 2(C_{11}^\theta + 2C_{12}^\theta + C_{44}^\theta). \quad (9)$$

In the last expression, a superscript θ is added to emphasize that isothermal elastic constants should be used for the initial strain, since the process for the initial compression is an isothermal one.

For the infinitesimal part of the deformation $[U']$ in (5), consider a travelling plane wave with a wave vector \mathbf{k}' in the initially deformed medium, the i 'th component can be expressed as

$$U_i' = B_i' \exp[i(\omega t - \mathbf{k}' \cdot \mathbf{x}')] \quad (10)$$

where B_i' is the i 'th component of the amplitude and

$$[x'] = [A'] [a'].$$

For a plane wave propagating along a general direction, the displacement vector B' may be neither parallel nor normal to the wave vector. From the matrix $[A']$ and the displacement U' , one can calculate the Jacobian, the Lagrangian strain η_{ij}' [Eq. (2)], and the stress tensor $[T']$ [Eq. (7)].

Substituting this $[T']$ into the equations of motion in an elastic medium

$$\sum_j \partial T_{ij}' / \partial x_j' = \rho_x \ddot{U}_i' \quad (11)$$

and neglecting the second- and the higher order terms of U' , one obtains a set of three equations for B_1' , B_2' , and B_3' which can be written in the following matrix form

$$[H] \begin{Bmatrix} B_1' \\ B_2' \\ B_3' \end{Bmatrix} = \rho_0 V^2 \begin{Bmatrix} B_1' \\ B_2' \\ B_3' \end{Bmatrix}, \quad (12)$$

where V is the phase velocity of a sound wave, and

$$V^2 = \omega^2 / |\mathbf{k}'|^2,$$

$[H]$ is a 3×3 matrix whose elements contain the second- and third-order elastic constants and the strains α_1 and α_2 .

For small strains one can consider the terms in $[H]$ containing α_i ($i=1, 2$) to be the perturbing terms. The problem is then to diagonalize $[H]$ to the zeroth order of α_i . The calculation is in general quite tedious but much simplified if pure modes exist.

For a wave propagating along $[\bar{1}\bar{1}0]$ direction (i.e., $2'$ axis) under a uniaxial compression applied in $[111]$ direction ($1'$ axis), the compressional wave is still a pure mode, since such a wave was originally a pure mode, and under this compression the stress does not alter the direction of the particle displacement. Hence, one may consider the following wave motion

$$\begin{aligned} U_2' &= B_2' \exp[i(\omega t - k_2' x_2')], \\ U_1' &= U_3' = 0. \end{aligned} \quad (13)$$

Substituting this into (11), one obtains one of the eigenvalues of $\rho_0 V^2$ [shown below in Eq. (14)].

The remaining operator which is now a 2×2 matrix can easily be diagonalized to the zeroth order of α_i by applying a unitary transformation with the unitary transform matrix constructed from the normalized eigenvectors of the unperturbed operator. For small strains such that the second-order terms of α_i can be neglected in the expression for $\rho_0 V^2$, the eigenvalues are readily found from the diagonal terms [see Eqs. (15) and (16)].

For waves propagating along $[\bar{1}\bar{1}2]$ direction the shear wave polarized in $[\bar{1}\bar{1}0]$ direction is still a pure mode under a compression in $[111]$ direction. The calculation resembles that for waves propagating along $[\bar{1}\bar{1}0]$ direction but is much more complicated. The expressions for $\rho_0 V^2$ are listed below [Eqs. (17)–(19)]. For convenience, the expressions of $\rho_0 V^2$ under hydrostatic pressure and under $[110]$ compression are also listed [Eqs. (20)–(26)].

(A) Uniaxial Compression in $[111]$ Direction

For compressional wave in $[\bar{1}\bar{1}0]$:

$$\begin{aligned} \rho_0 V_{22}^2 &= \frac{1}{2}(C_{11} + C_{12} + 2C_{44}) + \{-2(C_{11} + C_{12} + 2C_{44})\sigma \\ &\quad + \frac{1}{3}(C_{111} + 2C_{112})(1 - 2\sigma) - \frac{1}{6}(C_{111} - C_{123})(1 - 2\sigma) \\ &\quad + \frac{1}{3}C_{144}(1 - 2\sigma) - \frac{2}{3}C_{166}(1 + 4\sigma)\}\alpha_1. \end{aligned} \quad (14)$$

For shear wave in $[\bar{1}\bar{1}0]$ polarized in $[110]$:

$$\begin{aligned} \rho_0 V_{21}^2 &= \frac{1}{2}(C_{11} - C_{12}) + \{\frac{2}{3}(C_{11} - C_{12})(1 - 2\sigma) \\ &\quad + \frac{1}{6}(C_{111} - C_{123})(1 - 2\sigma)\}\alpha_1. \end{aligned} \quad (15)$$

For shear wave in $[\bar{1}\bar{1}0]$ polarized in $[001]$:

$$\begin{aligned} \rho_0 V_{212}^2 &= C_{44} + \frac{1}{3}\{2C_{44}(1 - 5\sigma) - 2C_{466}(1 + \sigma) \\ &\quad + C_{144}(1 - 2\sigma) + 2C_{166}(1 - 2\sigma)\}\alpha_1. \end{aligned} \quad (16)$$

For shear wave in $[\bar{1}\bar{1}2]$ polarized in $[\bar{1}\bar{1}0]$:

$$\begin{aligned} \rho_0 V_{32}^2 &= \frac{1}{6}(C_{11} - C_{12} + 4C_{44}) + \{-\frac{2}{3}(C_{11} - C_{12} + 4C_{44})\sigma \\ &\quad + (1/18)(C_{111} - C_{123})(1 - 2\sigma) - (4/9)C_{466}(1 + \sigma) \\ &\quad + \frac{2}{3}C_{144} - \frac{4}{3}C_{166}\}\alpha_1. \end{aligned} \quad (17)$$

For quasicompressional wave in $[\bar{1}\bar{1}2]$:

$$\begin{aligned} \rho_0 V_{33}^2 = & \frac{1}{12}(5C_{11} + C_{12} + 8C_{44} + R) \\ & + \left\{ \left[\frac{2}{3}s_{11}^2(C_{11} - C_{12} + C_{44})(1 - \sigma) - \frac{\sqrt{2}}{3}s_{11}s_{12}(C_{11} - C_{12} - 2C_{44})(1 - 3\sigma) - 2s_{12}^2(C_{11} + C_{12} + 2C_{44})\sigma \right] \right. \\ & + \frac{1}{3}s_{12}^2(C_{111} + 2C_{112})(1 - 2\sigma) + \left(\frac{1}{9}s_{11}^2 - \frac{\sqrt{2}}{9}s_{11}s_{12} - \frac{1}{6}s_{12}^2 \right) (C_{111} - C_{123})(1 - 2\sigma) + \left[- (2/9)s_{11}^2 - \frac{8}{9\sqrt{2}}s_{11}s_{12} \right] \\ & \times C_{456}(1 + \sigma) + \left[-\frac{1}{3}s_{11}^2(1 + 2\sigma) - \frac{4}{3\sqrt{2}}s_{11}s_{12}\sigma + \frac{1}{3}s_{12}^2(1 - 2\sigma) \right] C_{144} \\ & \left. + \left[\frac{2}{3}s_{11}^2 + \frac{4}{3\sqrt{2}}s_{11}s_{12}(1 - \sigma) - \frac{2}{3}s_{12}^2(1 + 4\sigma) \right] C_{166} \right\} \alpha_1. \quad (18) \end{aligned}$$

For quasishear wave in $[\bar{1}\bar{1}2]$ polarized in $[111]$:

$$\begin{aligned} \rho_0 V_{31}^2 = & \frac{1}{12}(5C_{11} + C_{12} + 8C_{44} - R) \\ & + \left\{ \left[\frac{2}{3}s_{12}^2(C_{11} - C_{12} + C_{44})(1 - \sigma) + \frac{\sqrt{2}}{3}s_{11}s_{12}(C_{11} - C_{12} - 2C_{44})(1 - 3\sigma) - 2s_{11}^2(C_{11} + C_{12} + 2C_{44})\sigma \right] \right. \\ & + \frac{1}{3}s_{11}^2(C_{111} + 2C_{112})(1 - 2\sigma) + \left(\frac{1}{9}s_{12}^2 + \frac{\sqrt{2}}{9}s_{11}s_{12} - \frac{1}{6}s_{11}^2 \right) (C_{111} - C_{123})(1 - 2\sigma) \\ & + \left[- (2/9)s_{12}^2 + \frac{8}{9\sqrt{2}}s_{11}s_{12} \right] C_{456}(1 + \sigma) + \left[-\frac{1}{3}s_{12}^2(1 + 2\sigma) + \frac{4}{3\sqrt{2}}s_{11}s_{12}\sigma + \frac{1}{3}s_{11}^2(1 - 2\sigma) \right] C_{144} \\ & \left. + \left[\frac{2}{3}s_{12}^2 - \frac{4}{3\sqrt{2}}s_{11}s_{12}(1 - \sigma) - \frac{2}{3}s_{11}^2(1 + 4\sigma) \right] C_{166} \right\} \alpha_1. \quad (19) \end{aligned}$$

Throughout, α_1 is the strain in the direction of the stress, $[111]$, σ is the Poisson ratio $-\alpha_2/\alpha_1$ where α_2 is the strain in any direction perpendicular to the $[111]$ direction. In addition,

$$s_{11} = \frac{1}{N} \frac{1}{3\sqrt{2}}(C_{11} - C_{12} - 2C_{44}), \quad (19a)$$

$$s_{12} = -\frac{1}{N} \frac{1}{12}(C_{11} + 5C_{12} + 4C_{44} + R), \quad (19b)$$

where

$$N = \{ (1/144)(C_{11} + 5C_{12} + 4C_{44} + R)^2 + (1/18)(C_{11} - C_{12} - 2C_{44})^2 \}^{1/2} \quad (19c)$$

$$R = \{ (C_{11} + 5C_{12} + 4C_{44})^2 + \frac{1}{8}(C_{11} - C_{12} - 2C_{44})^2 \}^{1/2}. \quad (19d)$$

(B) Hydrostatic Pressure

For compressional wave in $[100]$ ¹²⁻¹⁴:

$$\rho_0 V_1^2 = C_{11} + \{ C_{11}^\theta + 2C_{12}^\theta + 4C_{11} + C_{111} + 2C_{112} \} \alpha. \quad (20)$$

¹² Bhagavantam and Chelam (B-C) (Ref. 13) obtained expressions for the effective-elastic constants which were different from those obtained by Birch (Ref. 10). Two points in (B-C) derivation are subject to question. After corrections were made on them (Ref. 14) the (B-C) expressions agreed with those of Birch.

¹³ S. Bhagavatam and E. V. Chelam, Proc. Indian Acad. Sci. 25A, 1 (1960).

¹⁴ Z. P. Chang, Ph.D. thesis, Rensselaer Polytechnic Institute, Troy, New York, 1964 (unpublished).

For compressional wave in $[110]$:

$$\begin{aligned} \rho_0 V_2^2 = & \frac{1}{2}(C_{11} + C_{12} + 2C_{44}) \\ & + \{ C_{11}^\theta + 2C_{12}^\theta + 2(C_{11} + C_{12} + 2C_{44}) \\ & + (C_{111} + 2C_{112}) - \frac{1}{2}(C_{111} - C_{123}) \\ & + C_{144} + 2C_{166} \} \alpha. \quad (21) \end{aligned}$$

For shear wave in $[100]$ polarized in direction $\perp [100]$:

$$\rho_0 V_3^2 = C_{44} + \{ C_{11}^\theta + 2C_{12}^\theta + 4C_{44} + C_{144} + 2C_{166} \} \alpha. \quad (22)$$

For shear wave in $[110]$ polarized in $[\bar{1}\bar{1}0]$:

$$\begin{aligned} \rho_0 V_4^2 = & \frac{1}{2}(C_{11} - C_{12}) + \{ C_{11}^\theta + 2C_{12}^\theta \\ & + 2(C_{11} - C_{12}) + \frac{1}{2}(C_{111} - C_{123}) \} \alpha. \quad (23) \end{aligned}$$

For shear wave in $[110]$ polarized in $[001]$:

$$\rho_0 V_5^2 = C_{44} + \{ C_{11}^\theta + 2C_{12}^\theta + 4C_{44} + C_{144} + 2C_{166} \} \alpha. \quad (24)$$

(C) Uniaxial Compression in $[110]$ Direction

For compressional^{5,15} wave in $[001]$:

$$\begin{aligned} \rho_0 V^2 = & C_{11} + \{ -4\sigma_{001}C_{11} - \sigma_{001}C_{111} \\ & + (1 - \sigma_{110})C_{112} \} \alpha_1. \quad (25) \end{aligned}$$

¹⁵ A. Seeger and O. Buck, Z. Naturforsch. 15a, 1056 (1960).

For shear wave in $[\bar{1}\bar{1}0]$ polarized in $[\bar{1}10]$:

$$\rho_0 V^2 = \frac{1}{2}(C_{11} - C_{12}) + \left\{ (1 - \sigma_{110})(C_{11} - C_{12}) + \frac{1 - \sigma_{110}}{4} C_{111} - \frac{1 - \sigma_{110} + 2\sigma_{001}}{4} C_{112} + \frac{\sigma_{001}}{2} C_{123} \right\} \alpha_1, \quad (26)$$

where α_1 is the strain in the direction of the stress, $[\bar{1}10]$, σ_{001} and σ_{110} are the Poisson ratios for strains in $[001]$ and $[\bar{1}\bar{1}0]$ directions, respectively, under a stress in $[\bar{1}10]$ direction. Explicit expressions for these quantities follow:

$$\sigma_{001} = \frac{4C_{12}^\theta C_{44}^\theta}{C_{11}^\theta (C_{11}^\theta + C_{12}^\theta + 2C_{44}^\theta) - 2(C_{12}^\theta)^2}, \quad (27a)$$

$$\sigma_{110} = \frac{C_{11}^\theta (C_{11}^\theta + C_{12}^\theta - 2C_{44}^\theta) - 2(C_{12}^\theta)^2}{C_{11}^\theta (C_{11}^\theta + C_{12}^\theta + 2C_{44}^\theta) - 2(C_{12}^\theta)^2}. \quad (27b)$$

By measuring the velocities of sound wave under stress, one can evaluate the coefficients of α or α_1 in Eqs. (14)–(26) and solve for the third-order elastic constants.

III. MATERIALS AND APPARATUS

NaCl and KCl single crystals in the form of 1-in. cubes and with faces oriented approximately in the $[\bar{1}11]$, $[\bar{1}\bar{1}0]$, and $[\bar{1}\bar{1}2]$ crystallographic directions were supplied by the Harshaw Chemical Company. The orientation of the crystals was checked by the Laue back-reflection technique and the faces of the crystals were then ground to within $\pm \frac{1}{2}^\circ$ of the exact orientation. After one face was oriented, the opposite face was then ground parallel to the first one to within 0.00003 in. The dimensions of the specimen were measured with a supermicrometer (Pratt and Whitney) with a precision of 10μ in.

Ten-Mc/sec compressional and shear waves were generated, respectively, by $\frac{3}{8}$ -in. X -cut and Y -cut quartz transducers with an active circular area of $\frac{1}{4}$ in. in diameter. The transducers were bonded to the specimen by phenyl salicylate ("salol").

Velocity measurements were made with a pulsed ultrasonic interferometer¹⁶ constructed by Colvin.¹⁷ A brief description of this apparatus is given below.

Two pulses with a flat top of duration of 1μ sec are gated out from a 10 Mc/sec continuous sinusoidal wave. The time separation between the two pulses is variable from 3 to 10μ sec on one range and 4 to 40 on another range. The pulse height of the second pulse can be adjusted from 0.5 to 1.0 as large as the first one. The echoes of the pulses are picked up with the same transducer and displayed on an oscilloscope. For the appropriate time separation and ratio of pulse height,

¹⁶ J. Williams and J. Lamb, *J. Acoust. Soc. Am.* **30**, 308 (1958).

¹⁷ A. D. Colvin, Master's thesis, Rensselaer Polytechnic Institute, Troy, New York, 1959 (unpublished).

TABLE I. Temperature dependence of velocity of sound waves in NaCl and KCl together with the values of velocity. (All values are at 25°C).

Direction of propagation	Direction of polarization	Slope of vel. versus temp. (10^{-7} cm/ μ sec °C)	Velocity (cm/ μ sec)
NaCl $\rho_0 = 2.162$ g/cm ³			
$\bar{1}11$	$\bar{1}11$	-586	0.44163
$\bar{1}\bar{1}0$	$\bar{1}\bar{1}0$	-827	0.45058
$\bar{1}\bar{1}0$	$\bar{1}10$	-1477	0.29043
$\bar{1}\bar{1}0$	001	-177	0.24298
$\bar{1}\bar{1}2$	$\bar{1}\bar{1}2$	-903	0.45171
$\bar{1}\bar{1}2$	$\bar{1}11$	-988	0.27355
$\bar{1}\bar{1}2$	$\bar{1}\bar{1}0$	-659	0.25970
KCl $\rho_0 = 1.986$ g/cm ³			
$\bar{1}11$	$\bar{1}11$	-517	0.36679
$\bar{1}11$	$\bar{1}\bar{1}0$	-1116	0.25977
$\bar{1}11$	$\bar{1}\bar{1}2$	-1122	0.25941
$\bar{1}\bar{1}0$	$\bar{1}10$	-834	0.39014
$\bar{1}\bar{1}0$	$\bar{1}10$	-1453	0.29106
$\bar{1}\bar{1}0$	001	-100	0.17828
$\bar{1}\bar{1}2$	$\bar{1}\bar{1}2$	-1045	0.39809
$\bar{1}\bar{1}2$	$\bar{1}11$	-805	0.24656
$\bar{1}\bar{1}2$	$\bar{1}\bar{1}0$	-701	0.22408

cancellation between the second echo of the first pulse and the first echo of the second pulse occurs at discrete frequencies. From the values of these frequencies nearest to the resonant frequency of the quartz transducer one can obtain the acoustic velocities.¹⁷ According to the procedure of Williams and Lamb^{16,17} one includes by an iterative procedure a correction for the phase change arising at the quartz-specimen interface. Additional corrections for changes in transit path because of stress and temperature are also included.

The velocities measured in the room-temperature range were normalized to 25°C by the following equation:

$$V = V_T - \alpha_{vel}(T - 25), \quad (28)$$

where α_{vel} was the slope of the velocity versus temperature graph determined in the preliminary measurements for various modes in the room-temperature range under atmospheric pressure.

A uniaxial compression was applied to the sample through a cylindrical movable piston in a cylinder made of hard steel. The surfaces of the piston and the bottom of cylinder between which the samples were compressed were carefully surfaced and kept parallel. The stress was applied to the piston through a hand-operated mechanical press. The cage of the press was surrounded by foam insulators to reduce the temperature fluctuation, and a Cu-constantan thermocouple

TABLE II. Adiabatic second-order elastic constants of NaCl and KCl crystals at 25°C (in units of 10^{12} dyn/cm²).

	C_{11}	C_{12}	C_{44}
NaCl	0.4934	0.1293	0.1278
KCl	0.4076	0.0705	0.0632

FIG. 1. $\rho_0 V^2$ versus strain for shear wave in NaCl under stress [111]. Curve (A) for wave propagating in [112] and polarized in [111]. Curve (B) for wave propagating in [110] and polarized in [001]. Circles measured during increasing stress; crosses measured during decreasing stress.

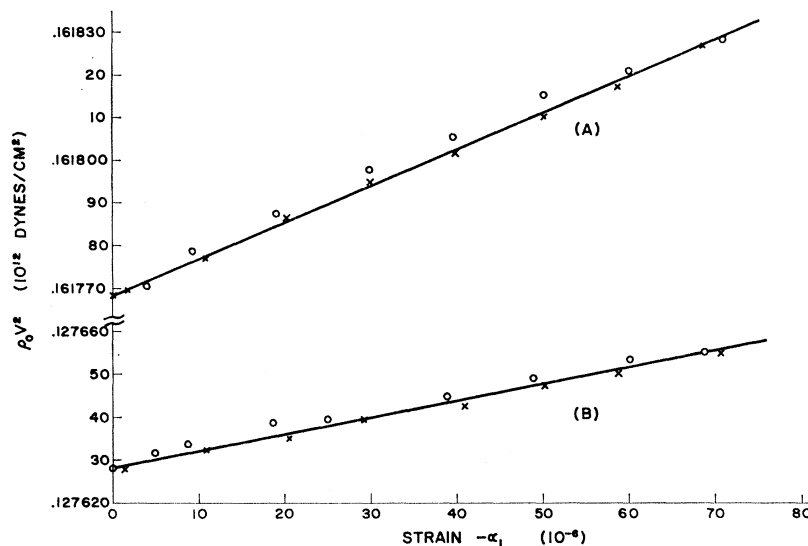


FIG. 2. $\rho_0 V^2$ versus strain for shear wave in KCl under stress [111]. Curve (A) for wave propagating in [112] and polarized in [111]. Curve (B) for wave propagating in [110] and polarized in [001]. Circles measured during increasing stress; crosses measured during decreasing stress.

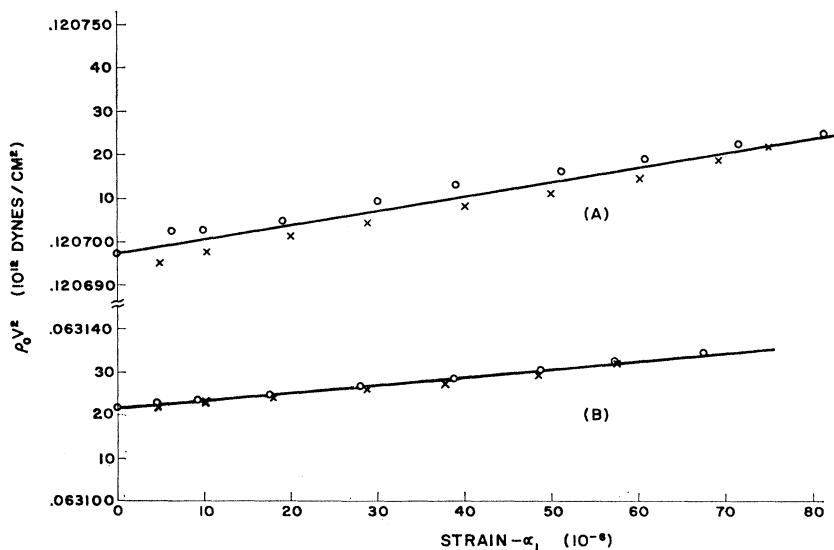


FIG. 3. $\rho_0 V^2$ versus strain for shear wave in KCl under stress [111] propagating in [110] and polarized in [110]. (A) Before plastic deformation. (●) Run 12 up; (×) Run 12 down; (○) Run 13 up. (B) After plastic deformation. (Δ) Run 13 down. (C) After plastic deformation (with the plastic strain excluded and using the thickness after the plastic deformation) (▲) Run 13 down.

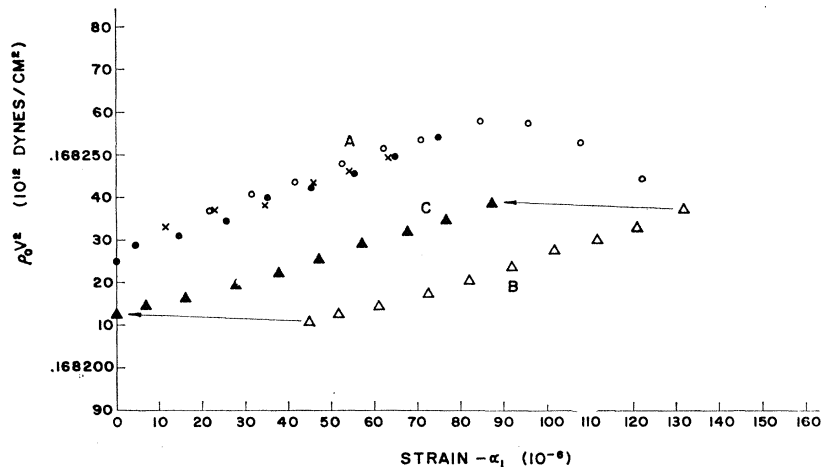


TABLE III. Slopes of $\rho_0 V^2$ -versus- $(-\alpha_1)$ graphs under uniaxial compression $\parallel [111]$.

	Mode		Slope of $\rho_0 V^2$ versus $(-\alpha_1)$ (10^{12} dyn/cm 2)			
	Direction of propagation	Direction of polarization	Measured values	NaCl Weighted average	Measured values	KCl Weighted average
V_{22}	$\bar{1}\bar{1}0$	$\bar{1}\bar{1}0$	0.4965 ^a	0.4965 ± 0.0091	0.4926 0.3938 0.4874 ^a	0.4485 ± 0.0231
$V_{2\bar{1}1}$	$\bar{1}\bar{1}0$	110	0.6839 0.6505	0.6558 ± 0.0087	0.3143 (R11) 0.3645 (R12 up) 0.3281 (R12 down) 0.3442 (R13 up) 0.3025 (R13 down)	0.3247 ± 0.0076
$V_{2\bar{2}2}$	$\bar{1}\bar{1}0$	001	0.3741 0.3698	0.3724 ± 0.0029	0.1830	0.1830 ± 0.0010
V_{32}	$\bar{1}\bar{1}2$	$\bar{1}\bar{1}0$	0.1792 0.1641 0.1538	0.1736 ± 0.0049	0.1231	0.1231 ± 0.0023
V_{33}	$\bar{1}\bar{1}2$	$\bar{1}\bar{1}2$	0.3137 ^a 0.3420	0.3234 ± 0.0067	0.4367	0.4367 ± 0.0048
V_{31}	$\bar{1}\bar{1}2$	111	0.9482 0.8537	0.8706 ± 0.0303	0.3354	0.3354 ± 0.0032

^a Velocity measurements were made with cancellation between the third echo of the first pulse against the first echo of the second pulse in order to obtain sharper cancellation.

together with a Reeds and Northrup K-3 potentiometer were used to measure the temperature to 0.01°C.

The strain in the direction of the applied stress was measured with SR-4 strain gauges of type A-7 (Baldwin-Lima-Hamilton Corporation). Two pairs of strain gauges were bonded on the opposite $\{110\}$ faces of the specimens. The two gauges on the same side were connected in series to give an average strain of that side. The readings of the strain on both sides were averaged to give the average strain of the specimen. In a typical run, the difference between the strains on both sides was less than 10% for a maximum strain of 70×10^{-6} . Each pair of the strain gauges on the opposite faces of the sample forms an arm of the two ac bridges in the two-channel recorder.

TABLE IV. Slopes of $\rho_0 V$ -versus- $(-\alpha_1)$ graphs for NaCl under uniaxial compression $\parallel [110]$.

	Mode		Slope of $\rho_0 V^2$ versus $(-\alpha_1)$ graph (10^{12} dyn/cm 2)	
	Direction of propagation	Direction of polarization	Measured values	Weighted average
V_{33}'	001	001	-1.627 -1.467	-1.564 ± 0.053
$V_{2\bar{1}1}'$	$\bar{1}\bar{1}0$	110	+1.338 1.068 1.371 1.199	+1.218 ± 0.052

A dummy sample with the same type of strain gauges and the same connections was used as a control. Each pair of strain gauges on this dummy forms the other arm in an ac bridge, and balances the corresponding pair of gauges on the test specimen. The dummy sample was kept at the same temperature as the specimen to eliminate the effect of temperature change on the reading of the strain.

IV. MEASUREMENTS

The temperature dependence of the velocities for various modes in NaCl and KCl obtained in preliminary measurements together with the values of velocity at $T=25^\circ\text{C}$ are listed in Table I. In the correction for the thermal expansion, the following coefficients of

TABLE V. Slopes of $\rho_0 V^2$ -versus- $(-\alpha)$ graphs under hydrostatic pressure (calculated from Lazarus' data).

	Mode		Slope of $\rho_0 V^2$ versus $(-\alpha)$ graph (10^{12} dyn/cm 2)	
	Direction of propagation	Direction of polarization	NaCl	KCl
	V_1	100	100	+7.2838+0.0730
V_2	110	110	+3.7832 \pm 0.0813	+2.5786 \pm 0.0417
V_3	100	\perp 100	-0.1597 \pm 0.0011	-0.4195 \pm 0.0020
V_4	110	110	+2.8361 \pm 0.0093	+2.4683 \pm 0.0134
V_5	110	001	-0.1956 ^a	-0.4325 \pm 0.0025

^a From the first two measurements.

TABLE VI. Values of s_{11}^2 , $2s_{11}s_{12}$, s_{12}^2 and the Poisson ratios σ , σ_{001} , and σ_{110} .

	Expressions (19a) to (19d)		Calculated value		
			NaCl	KCl	
s_{11}^2			0.00843	0.06895	
$2s_{11}s_{12}$			-0.18287	-0.50674	
s_{12}^2			0.99157	0.93105	
σ	Direction of stress 111	Direction of strain $\perp 111$	$\frac{C_{11}^{\theta}+2C_{12}^{\theta}-2C_{44}^{\theta}}{2(C_{11}^{\theta}+2C_{12}^{\theta}+C_{44}^{\theta})}$	0.271	0.337
σ_{110}	110	$\bar{1}\bar{1}0$	$\frac{C_{11}^{\theta}(C_{11}^{\theta}+C_{12}^{\theta}-2C_{44}^{\theta})-2(C_{12}^{\theta})^2}{C_{11}^{\theta}(C_{11}^{\theta}+C_{12}^{\theta}+2C_{44}^{\theta})-2(C_{12}^{\theta})^2}$	0.155	0.068
σ_{001}	110	001	$\frac{4C_{12}^{\theta}C_{44}^{\theta}}{C_{11}^{\theta}(C_{11}^{\theta}+C_{12}^{\theta}+2C_{44}^{\theta})-2(C_{12}^{\theta})^2}$	0.357	0.554

TABLE VII. Linear combinations of C_{ijk} for NaCl. The equations are to be read horizontally, e.g., for V_{212} , $0.8474C_{456}-0.1526C_{144}-0.3053C_{166}=0.3421$.

Under [111] compression:							
	$C_{111}+2C_{112}$	$C_{111}-C_{123}$	C_{456}	C_{144}	C_{166}	= Slope-2nd-order terms	
V_{22} :	-0.1526	+0.0763	0	-0.1526	+1.3895	+0.0204±0.0110 (29)	
V_{211} :	0	-0.0763	0	0	0	+0.7670±0.0091 (30)	
V_{212} :	0	0	+0.8474	-0.1526	-0.3053	+0.3421±0.0033 (31)	
V_{32} :	0	-0.0254	+0.5649	-0.6667	+0.3614	+0.0154±0.0056 (32)	
V_{33} :	-0.1513	+0.0687	-0.0707	-0.1704	+1.4350	-0.1458±0.0112 (33)	
V_{31} :	-0.0013	-0.0432	+0.3531	+0.5318	-0.7122	+1.1027±0.0321 (34)	
Under [110] compression:							
	C_{111}	C_{112}	C_{123}	C_{456}	C_{144}	C_{166}	= Slope-2nd-order terms
V_{33}' :	+0.1551	-0.6427	0	0	0	0	-1.869±0.053 (35)
V_{211}' :	-0.1607	+0.2382	-0.0775	0	0	0	+1.452±0.052 (36)
Under hydrostatic pressure (calculated from Lazarus' data):							
	$C_{111}+2C_{112}$	$C_{111}-C_{123}$	C_{144}	C_{166}		= Slope-2nd-order terms	
V_1 :	-1	0	0	0		+9.9668±0.0730 (37)	
V_2 :	-1	$\frac{1}{2}$	-1	-2		+6.2460±0.0813 (38)	
V_3 :	0	0	-1	-2		+1.0608±0.0011 (39)	
V_4 :	0	$-\frac{1}{2}$	0	0		+4.2738±0.0093 (40)	
V_5 :	0	0	-1	-2		+1.025 (41)	

TABLE VIII. Linear combinations of C_{ijk} for KCl.

Under [111] compression:						
	$C_{111}+2C_{112}$	$C_{111}-C_{123}$	C_{456}	C_{144}	C_{166}	= Slope-2nd-order terms
V_{22} :	-0.1084	+0.0542	0	-0.1084	+1.5664	+0.0405±0.0231 (29')
V_{211} :	0	-0.0542	0	0	0	+0.3978±0.0076 (30')
V_{212} :	0	0	+0.8916	-0.1084	-0.2168	+0.1540±0.0010 (31')
V_{32} :	0	-0.0181	+0.5944	-0.6667	+0.4499	-0.0096±0.0023 (32')
V_{33} :	-0.1009	+0.0350	-0.1925	-0.1430	+1.5707	+0.0688±0.0048 (33')
V_{31} :	-0.0075	-0.0170	+0.4897	+0.5929	-0.6710	+0.4722±0.0032 (34')
Under hydrostatic pressure (calculated from Lazarus's data):						
	$C_{111}+2C_{112}$	$C_{111}-C_{123}$	C_{144}	C_{166}		= Slope-2nd-order terms
V_1 :	-1	0	0	0		+7.3477±0.0514 (37')
V_2 :	-1	$\frac{1}{2}$	-1	-2		+4.3079±0.0417 (38')
V_3 :	0	0	-1	-2		+0.3535±0.0020 (39')
V_4 :	0	$-\frac{1}{2}$	0	0		+3.6625±0.0134 (40')
V_5 :	0	0	-1	-2		+0.3405±0.0025 (41')

linear thermal expansion obtained from Henglein's measurements¹⁸ were used:

$$\begin{array}{cc} \text{NaCl} & \text{KCl} \\ (115/3) \times 10^{-6}/^\circ\text{C} & (110/3) \times 10^{-6}/^\circ\text{C} \end{array}$$

The adiabatic second-order elastic constants at 25°C are determined from the $\rho_0 V^2$ of the pure modes using the method of least squares. Their values are shown in Table II. Except C_{12} of NaCl, these values agree with Lazarus' values to within half a percent. For C_{12} the difference is about 6%.

The velocities of ultrasonic waves propagating along the $[1\bar{1}0]$ and $[\bar{1}12]$ directions under a uniaxial compression in $[111]$ were measured as functions of strain. After corrections had been made for the deformation and the thermal expansion, and the velocities were normalized to 25°C using Eq. (28), the values of $\rho_0 V^2$ were plotted against the strain ($-\alpha_1$) in the direction of the stress. Several typical graphs of such plots are shown in Figs. 1–3 for NaCl and KCl. In these measurements, data were taken during the process of increasing and decreasing stress, as indicated, respectively, by circles and crosses in the graphs. The curves of $\rho_0 V^2$ versus strain are quite linear. One of the runs shows the effect of plastic deformation (Fig. 3).

The KCl sample was compressed to a strain of 75×10^{-6} during the velocity measurement, the load was next reduced to the weight of the piston and then increased again. After a strain of about 90×10^{-6} drastic deformation occurred, and the calculated velocity drops as no account was taken of the change of the path length with plastic deformation. After the specimen was unloaded, the residual plastic strain was 45×10^{-6} . The strain was then recalculated excluding the permanent set, and the thickness remeasured after the transducers were removed. The $\rho_0 V^2$ as function of the recalculated strain is shown on the same graph [curve (C)]. The weighted average of the slope before the plastic deformation is 0.3384 with a standard deviation σ of 0.0105. The slope after the plastic deformation is 0.3025. Since this value is beyond the lower 3σ limit, 0.3069, the difference in the slope before and after the plastic deformation appears to be significant. The effect is probably caused by the dislocations generated in plastic deformation. The effect of dislocations on the third-order elastic constants has also been observed by Hikata *et al.*,¹⁹ in the harmonic generation of ultrasonic waves in aluminum.

It is tempting to conclude that the lower of $\rho_0 V^2$ curve by plastic deformation is also a dislocation effect but some systematic error could also have been introduced in the length measurement after removing the transducer and bonding material.

A summary of the slopes of $\rho_0 V^2$ -versus- $(-\alpha_1)$ graphs for various modes of propagation in NaCl and KCl

under uniaxial compression in $[111]$ direction is shown in Table III. For the uniaxial compression in $[110]$, the results for NaCl are shown in Table IV; no measurements were made on KCl under such a compression.

Lazarus has measured the velocities of sound waves in NaCl and KCl under hydrostatic pressure. From his data,⁶ the quantity $\rho_0 V^2$ can be calculated and plotted against the strain ($-\alpha$). The slopes of $\rho_0 V^2$ versus ($-\alpha$) thus obtained are listed in Table V.

V. RESULTS AND DISCUSSION

A. The Linear Combinations of the Third-Order Elastic Constants

From the adiabatic (Table I) and isothermal (Appendix) second-order elastic constants, the values of s_{11} , s_{12} , σ , σ_{110} , σ_{001} can be calculated. They are listed in Table VI to be substituted in Eqs. (14)–(26). By equating the coefficients of ($-\alpha_1$) in these equations to the slopes of $\rho_0 V^2$ -versus- $(-\alpha_1)$ graphs, one obtains sets of linear simultaneous equations for the determination of the third-order elastic constants. These coefficients for these equations are shown in Table VII for NaCl [Eqs. (29)–(41)] and Table VIII for KCl [Eqs. (29')–(41')].

Before solving these equations, we shall check their internal consistency.

B. Internal Check among the Measurements under $[111]$ Compression

From the coefficients of ($-\alpha_1$) in the Eqs. (14)–(19), one can show that (33) and (34) can be expressed in terms of Eqs. (29) to (32) [Table VII] as

$$\begin{aligned} \text{Eq. (33)} = & (29) \times s_{12}^2 + (30) \times \left(s_{11}^2 - \frac{s_{11}s_{12}}{\sqrt{2}} \right) \\ & + (31) \times \left(s_{11}^2 + \frac{2s_{11}s_{12}}{\sqrt{2}} \right) + (32) \\ & \times \left(-s_{11}^2 - \frac{1}{\sqrt{2}} s_{11}s_{12} \right), \quad (42) \end{aligned}$$

$$\begin{aligned} \text{Eq. (34)} = & (29) \times s_{11}^2 + (30) \times \left(s_{12}^2 + \frac{s_{11}s_{12}}{\sqrt{2}} \right) \\ & + (31) \times \left(s_{12}^2 - \frac{2s_{11}s_{12}}{\sqrt{2}} \right) + (32) \\ & \times \left(-s_{12}^2 + \frac{1}{\sqrt{2}} s_{11}s_{12} \right). \quad (43) \end{aligned}$$

Hence there are two internal checks. Same relationships also hold for Eqs. (29') to (34') [Table VIII] for KCl.

¹⁸ F. A. Henglein, Z. Phys. Chem. **115**, 91 (1925).

¹⁹ A. Hikata, B. B. Chick, and C. Elbaum, Appl. Phys. Letters **3**, 195 (1963).

For the measurements on NaCl, the right side of (42) is 0.0341 ± 0.0103 while the left side is -0.1458 ± 0.0067 ; the right side of (43) is 1.076 ± 0.0166 while the left side is 1.103 ± 0.0303 . For the measurements on KCl, the right side of (42) is 0.0908 ± 0.0309 while the left side is 0.0688 ± 0.0048 ; the right side of (43) is 0.5111 ± 0.0100 while the left side is 0.4722 ± 0.0032 .

It can be seen from these internal checks that the measurements on KCl under [111] compression are reasonably consistent. The difference is within the limit of three times the standard deviation. For NaCl one of the internal checks (42) is poorly satisfied and it is thought that the blame lies with the V_{22} measurement. In this measurement the output impedance of the gate circuit and the cable were improperly matched and hence the input signal to the transducer was very small. This mismatching was remedied for the other subsequent measurements and a considerably larger S/N ratio was obtained which enabled more accurate measurements.

C. Internal Check among the Measurements under Hydrostatic Pressure

Among the five equations (37) to (41), only three are linearly independent. Hence there are two internal checks. It can be shown that

$$\text{Eq. (38)} = \text{Eq. (37)} - \text{Eq. (40)} \\ + [\text{Eq. (39) or (41)}]. \quad (44)$$

Same relationship also holds for Eqs. (37') to (41') for KCl.

From Lazarus' data for NaCl (Table VII), the right side of (44) using (39) is 6.754 ± 0.083 , or using (41) is 6.719 , while the left side is 6.246 ± 0.081 ; for KCl (Table VIII), the right side using (39) is 4.039 ± 0.066 , or using (41) is 4.026 ± 0.067 , while the left side is 4.308 ± 0.042 . The discrepancies are all within the limit of three times the standard deviation.

D. Determination of the Five Third-Order Elastic Constants

From the measurements under [111] compression and those under hydrostatic pressure by Lazarus, five third-order elastic constants can be determined. A preliminary question is how to weight these two sets of equations.

For NaCl the averaged probable error in the data for the [111] compression (Table III) is about $\frac{1}{4}$ of that in the data for the hydrostatic compression (Table IV). For KCl it is about $\frac{1}{3}$. Hence, in solving for the elastic constants, we shall weight the set of equations for NaCl under [111] compression by 4 against the set under the hydrostatic pressure. For KCl, the corresponding set will be weighted by 3.

The values of the five third-order elastic constants

TABLE IX. Values of the five third-order elastic constants for NaCl and KCl at 25°C (10^{12} dyn/cm²).

	$C_{111} + C_{112}$	$C_{111} - C_{123}$	C_{456}	C_{144}	C_{166}
NaCl	-9.91 ± 0.04	-9.10 ± 0.08	0.271 ± 0.014	0.257 ± 0.016	-0.611 ± 0.007
KCl	-7.44 ± 0.01	-7.15 ± 0.02	0.118 ± 0.004	0.127 ± 0.005	-0.245 ± 0.002

determine from these weighted equations using the method of least squares are shown in Table IX.

For the purpose of comparison, calculations in which the set of equations under [111] compression was weighted by 1 and 10 were also made. The largest shifts were about 8% in $C_{111} - C_{123}$ for NaCl and 18% in C_{144} for KCl. For the other constants, the shifts were less than 6%.

From the values of C_{456} and C_{144} , it can be seen that one of the Cauchy relations for third-order constants, $C_{456} = C_{144}$, is satisfied to within the probable error for both NaCl and KCl crystals at room temperature.

E. Evaluation of the Six Third-Order Elastic Constants

Since from the measurements under the [111] and hydrostatic compressions only five third-order elastic constants can be determined, an effort was made to obtain other independent equations by making measurements under a uniaxial compression applied in the [110] direction.

Unfortunately, when such a compression is applied, the resolved shear stress in the easy-slip direction of dislocations in the slip planes does not vanish, and plastic deformation sets in easily and affects the measurements. Moreover, it can be seen from Eqs. (35) and (36) for the [110] compression that the numbers on the right side are much larger than the coefficients on the left side. A slight fluctuation in the measurement affects the final result of the six third-order elastic constants very much. For example, on the right side of Eq. (36) a change from 1.45 to 1.30 (which is within the limit of three times the standard deviation for measurements under this compression) causes the resulting C_{112} to change from 0.29 to -0.50 and the resulting C_{123} from -0.413 to $+0.014$. Hence the data obtained from the [110] compression were not used in the evaluation of the third-order elastic constants. However, they can serve as a check to the evaluation by another method as will be described below.

Since the Cauchy relation $C_{456} = C_{144}$ is satisfied to within the probable error we shall assume the validity of the other two Cauchy relations $C_{123} = C_{456}$ and $C_{112} = C_{166}$, although this assumption is open to some question because, as Nran'yan²⁰ has shown, only the relation

²⁰ A. A. Nran'yan, Fiz. Tverd. Tela **5**, 177 (1963) [English transl.: Soviet Phys.—Solid State **5**, 129 (1964).]

TABLE X. Comparison between experimental and theoretical values of C_{ijk} and their combinations at 25°C (in Brugger's definition of C_{ijk} and in units of 10^{12} dyn/cm²). Parenthetical values are the ones estimated by assuming the Cauchy relations.

	NaCl		KCl	
	Expt.	Theoret.	Expt.	Theoret.
C_{111}	(-8.80)	-5.45	(-7.01)	-5.07
C_{112}	(-0.571)	-0.688	(-0.224)	-0.458
C_{123}	(0.284)	0.269	(0.133)	0.148
$C_{111}+2C_{112}$	-9.91	-6.83	-7.44	-5.99
$C_{111}-C_{123}$	-9.10	-5.72	-7.15	-5.22
C_{456}	0.271	0.325	0.118	0.207
C_{144}	0.257	0.325	0.127	0.207
C_{166}	-0.611	-0.63	-0.245	-0.40

$C_{456}=C_{144}$ can be expected to hold at all temperatures even for a central force model. The other two equalities hold only at 0°K. However, we shall use these relations to estimate the values of C_{111} , C_{112} , and C_{123} at room temperature. From the results in Table IX,

$$C_{111}+2C_{112} = \begin{matrix} \text{(For NaCl)} \\ -9.91 \end{matrix} \quad \begin{matrix} \text{(For KCl)} \\ -7.44 \end{matrix} \quad (45)$$

$$C_{111}-C_{123} = \begin{matrix} -9.10 \\ -7.15 \end{matrix} \quad (46)$$

If we assume

$$C_{123}=\frac{1}{2}(C_{456}+C_{144})= \begin{matrix} 0.264 \\ 0.123 \end{matrix} \quad (47)$$

$$C_{112}=C_{166} = \begin{matrix} -0.611 \\ -0.245 \end{matrix}, \quad (48)$$

then we can check the consistency of these equations.

The relation relating these four equations is

$$\text{Eq. (45)}-2\times\text{Eq. (48)}=\text{Eq. (46)}+\text{Eq. (47)}. \quad (49)$$

For NaCl, the left side of (49) is -8.69 while the right side is -8.84; for KCl, the left side is -6.95 while the right side is -7.03. Hence the introduction of the other two Cauchy relations does not cause appreciable inconsistency among these equations. Using the method of least squares, one can obtain the estimated values of C_{111} , C_{112} , and C_{123} from the four equations (45) to (48). The results are shown parenthetically in Table X.

Using these estimated values, one can check the results obtained from the [110] compression in NaCl. For V_{33}' one obtains -1.00 for the left side of Eq. (35) while the value on the right side obtained through the experiment is -1.87. For V_{211}' , one obtains 1.25 for the left side of Eq. (36) while the value on the right side is 1.45. Although the value for V_{211}' are rather close, the discrepancy in V_{33}' is quite large. This indicates that the internal consistency in the measurements under the [110] compression is poor. This may be caused by the dislocation contribution to the third-order elastic constants and also the small range of strain which reduced the accuracy of the measurements.

G. Comparison with Theory

While this experiment was underway, Nran'yan²⁰ published values of the third-order elastic constants of

NaCl-type alkali halide crystals. He used the Born-Mayer model in which the potential energy between two particles was represented by the following expression:

$$\phi_{\mu\nu}R_{\mu\nu}^{m0}=(\pm)_{\mu\nu}e^2/R_{\mu\nu}^{m0}+B_{\mu\nu}\exp(-R_{\mu\nu}^{m0}/b_{\mu\nu}),$$

where $R_{\mu\nu}^{m0}$ is the distance between the equilibrium positions of the μ th particle in the m th cell and the ν th particle in the 0th cell in the deformed lattice, e is the electronic charge, $b_{\mu\nu}$ and $B_{\mu\nu}$ are two constants describing the repulsion and

$$\begin{aligned} (\pm)_{\mu\nu} &= + \text{ when } \mu = \nu \\ &= - \text{ when } \mu \neq \nu. \end{aligned}$$

The first term represents the contribution from the Coulomb interaction and the second represents the repulsion of their electron shells.

The theoretical values of the third-order elastic constants and their linear combinations at room temperature are listed in Table X together with the present experimentally determined values. It is seen that the sign and the order of magnitude of the theoretically predicted values agree with experiment although quantitative agreement is lacking.

VI. CONCLUSIONS

The relations between the velocities of sound waves propagating along the [110] and [112] directions in a cubic lattice of high symmetry under a uniaxial compression applied in [111] direction were derived. The velocities of ultrasonic waves were measured at room temperature as functions of the strain using the pulsed-ultrasonic interference technique. From the measurements under the [111] compression and those under hydrostatic pressure, the values of five combinations of third-order elastic constants of NaCl and KCl at room temperature were obtained. It is seen that the Cauchy relation $C_{456}=C_{144}$ is satisfied to within the probable error for both NaCl and KCl single crystals at room temperature. By assuming the validity of the other two Cauchy relations, one can estimate the values of C_{111} , C_{112} , and C_{123} . The theoretical values predicted by Nran'yan were compared with the experiment. Although the sign and order of magnitude agree quite well, some discrepancies exist between the values.

ACKNOWLEDGMENTS

The author wishes to express his sincere gratitude to Professor H. B. Huntington for suggesting the problem and for his many enlightening discussions and guidance throughout the course of this work. The author is also indebted to Professor J. L. Katz for the use of the x-ray equipment and the IBM 1620 computer, and to Professor R. H. Trathen for his helpful advice in the measurement of strain and the use of the equipment.

APPENDIX: ADIABATIC AND ISOTHERMAL SECOND-ORDER ELASTIC CONSTANTS

For infinitesimal strains, it has been shown²¹ that the differences between the adiabatic and isothermal elastic constants are

$$\begin{aligned} C_{11}^{\sigma} - C_{11}^{\theta} &= C_{12}^{\sigma} - C_{12}^{\theta} = \alpha^2 (C_{11} + 2C_{12})^2 T / \rho C_v, \\ C_{44}^{\sigma} - C_{44}^{\theta} &= 0, \end{aligned}$$

where α is the linear thermal expansion coefficient, T is

²¹ W. P. Mason, *Piezoelectric Crystals and Their Application to Ultrasonics* (Van Nostrand Publishing Company, Princeton, New Jersey, 1948).

the absolute temperature and C_v is the specific heat at constant volume. For NaCl at $T=300^\circ\text{K}$, $\alpha=38.3 \times 10^{-6}/^\circ\text{C}$, $C_{11}+2C_{12}=0.752 \times 10^{12}$ dyn/cm² and $\rho=2.162$ g/cm³. With $C_v=0.811$ J/g $^\circ\text{C}$, one obtains $C_{11}^{\sigma}-C_{11}^{\theta}=0.0142 \times 10^{12}$ dyn/cm². From the values of C_{ij}^{σ} in Table II, one obtains $C_{11}^{\theta}=0.4792$, $C_{12}^{\theta}=0.1151$ (10^{12} dyn/cm²). For KCl at $T=300^\circ\text{K}$, $\alpha=36.7 \times 10^{-6}/^\circ\text{C}$, $C_{11}+2C_{12}=0.549 \times 10^{12}$ dyn/cm² and $\rho=1.986$ g/cm³. With $C_v=0.644$ J/g $^\circ\text{C}$, one obtains $C_{11}^{\sigma}-C_{11}^{\theta}=0.0095 \times 10^{12}$ dyn/cm². From the values of C_{ij}^{σ} in Table II, one obtains $C_{11}^{\theta}=0.3981$, $C_{12}^{\theta}=0.0610$ (10^{12} dyn/cm²).

Anisotropic Dispersive Continuum Model for Lattice Dynamics of Solids. III. Electrical and Thermal Resistivities of Sodium

K. C. SHARMA AND S. K. JOSHI*

Physics Department, Allahabad University, Allahabad, India

(Received 28 June 1965)

A calculation of the electrical and thermal resistivities of sodium is carried out within the free-electron approximation and using the anisotropic-dispersive-continuum model for the lattice dynamics of the metal. The temperature dependence of these resistivities is calculated and results are compared with experiments. The calculated values of the resistivities exceed the experimental values at low temperatures, and at higher temperature there are again discrepancies.

I. INTRODUCTION

THE problem of transport properties of metals, which is very basic to the solid-state theory, is by no means a straightforward one, and has attracted regular attention since 1928, when Bloch¹ first gave a theory explaining the qualitative features of the electrical resistivity of solids. Since alkali metals have the simplest electronic structure they are the favorites of the theorists. The most satisfactory approach to date is that of Bardeen² and his results for the electrical resistivity of monovalent metals are in reasonable agreement with experiment. Bardeen assumes the electronic behavior to be free-electron-like and adopts the Debye approximation for the phonon spectrum. In recent years attempts have been made to improve upon these approximations. Baily³ was the first to rid the theory of the Debye model and use a Born-von Kármán model for the dynamics of ions. He evaluated the force constants from the elastic constants and found the lattice waves to exhibit highly anisotropic behavior. Darby and March⁴ have directly used the

experimentally measured dispersion curves for phonons in sodium to calculate the electrical resistivity and Darby⁵ has used the same approach to compute the thermal resistivity of sodium. They have also accounted for exchange and correlation. Collins and Ziman⁶ have shown a way to calculate the electron-phonon matrix element for a distorted Fermi surface by using their "12-cone approximation." They, however, use the Debye approximation for the phonons. Hasegawa⁷ has amalgamated the procedures of Baily, and Collins and Ziman. He takes account of both the phonon spectrum and the electronic band structure. Bross and Holz⁸ have also reported a calculation of the electrical resistivity of alkali metals taking into account both the electronic structure and the phonon spectrum. Very recently, Greene and Kohn⁹ have made a theoretical study of the electrical resistivity of solid and liquid sodium which seems to be quite rigorous and convincing. Although the calculation is believed to incorporate accurately many-body effects, umklapp processes, time-dependent effects, etc., and they utilize the inelastic-neutron-scattering data to obtain information

* Present address: Physics Department, University of California, Riverside, California.

¹ F. Bloch, *Z. Physik*, **52**, 555 (1928).

² J. Bardeen, *Phys. Rev.* **52**, 688 (1937).

³ M. Baily, *Phys. Rev.* **120**, 381 (1960).

⁴ J. K. Darby and N. H. March, *Proc. Phys. Soc. (London)* **84**, 591 (1964).

⁵ J. K. Darby (private communication).

⁶ J. G. Collins and J. M. Ziman, *Proc. Roy. Soc. A* **264**, 60 (1961).

⁷ A. Hasegawa, *J. Phys. Soc. Japan* **19**, 504 (1964).

⁸ H. Bross and A. Holz, *Phys. Status Solidi* **3**, 1141 (1963).

⁹ M. P. Greene and W. Kohn, *Phys. Rev.* **137**, A513 (1965).